

Research Article

## Biodegradable m-PEG/PCL Core-Shell Micelles: Preparation and Characterization as a Sustained Release Formulation for Curcumin

Hossein Danafar<sup>1,2,3</sup>, Soodabeh Davaran<sup>1\*</sup>, Kobra Rostamizadeh<sup>2,3</sup>, Hadi Valizadeh<sup>4</sup>, Mehrdad Hamidi<sup>3,5</sup>

<sup>1</sup> Faculty of Pharmacy, Tabriz University of Medical Sciences, Tabriz, Iran.

<sup>2</sup> Zanjan Pharmaceutical Nanotechnology Research Center, Zanjan University of Medical Sciences, Zanjan, Iran.

<sup>3</sup> Department of Medicinal Chemistry, School of Pharmacy, Zanjan University of Medical Sciences, Zanjan, Iran.

<sup>4</sup> Department of Pharmaceutics, School of Pharmacy, Tabriz University of Medical Sciences, Tabriz, Iran.

<sup>5</sup> Department of Pharmaceutics, School of Pharmacy, Zanjan University of Medical Sciences, Zanjan, Iran.

### Article info

#### Article History:

Received: 6 January 2014

Revised: 30 January 2014

Accepted: 1 February 2014

ePublished: 31 December 2014

#### Keywords:

- mPEG-PCL
- Micelles
- Curcumin
- Drug delivery

### Abstract

**Purpose:** Among the potent anticancer agents, curcumin is known as a very efficacious against many different types of cancer cells, but its clinical applications has been limited because of hydrophobicity, low gastrointestinal absorption, poor bioavailability and rapid metabolism. In this way, a novel micellar delivery system with mPEG-PCL was synthesized and the release profile of the curcumin from the drug-loaded micelles was evaluated.

**Methods:** In this study, curcumin was encapsulated within monomethoxypoly(ethylene glycol)-poly( $\epsilon$ -caprolactone) (mPEG-PCL) micelles through a single-step nano-precipitation method, leading to creation of curcumin-loaded mPEG-PCL (Cur/mPEG-PCL) micelles. Di-block mPEG-PCL copolymers were synthesized and used to prepare micelles. mPEG-PCL copolymer was characterized *in vitro* by HNMR, FTIR, DSC and GPC techniques. Then, mPEG-PCL copolymers with curcumin were self-assembled into micelles in aqueous solution. The resulting micelles were characterized further by various techniques such as dynamic light scattering (DLS) and atomic force microscopy (AFM).

**Results:** The findings showed the successful formation of smooth and spherical curcumin-loaded micelles. The encapsulation efficiency of curcumin was  $88 \pm 3.32\%$ . The results of AFM revealed that the micelles have spherical shapes with size of 73.8 nm. The release behavior of curcumin from micelles was compared in different media. *In vitro* release of curcumin from curcumin-entrapped micelles was followed remarkably sustained profile. The sustained release of drug was hypothetically due to the entrapment of curcumin in core of micelles.

**Conclusion:** The results indicate the successful formulation of curcumin loaded m-PEG/PCL micelles. From the results, it can be concluded that curcumin m-PEG-PCL micelles may be considered as an effective treatment strategy for cancer in the future.

### Introduction

Curcumin is the yellowish pigmentation of turmeric (*Curcuma longa* L.) which is widely used as a food flavoring and coloring agent. Its chemical formula 1,7-bis(4-hydroxy-3-methoxyphenyl)-1,6-heptadiene-3,5-dione with a chemical structure in the keto-enol tautomerism. Curcumin is an interesting therapeutic agent from a pharmaceutical point of view because of its remarkable biological properties, including its antioxidant, antimicrobial, anti-inflammatory, and wound healing activities.<sup>1-4</sup> It also exhibits potential use for the medicinal treatment of various diseases, especially cancer.<sup>5-7</sup> Nevertheless, curcumin suffers from some drawbacks including low water solubility under acidic or neutral conditions, high decomposition rate in an alkaline media, and photodegradation in organic solvents which subsequently limit its clinical applications.<sup>8,9</sup> Because of these shortcomings, many attempts to increase the

solubility and stability of curcumin have been reported, e.g. the use of curcumin nanoparticles,<sup>10</sup> the inclusion of curcumin into central cavities of cyclodextrins,<sup>11,12</sup> the use of curcumin-encapsulated microemulsions,<sup>13</sup> and curcumin-loaded O-carboxymethyl chitosan nanoparticles<sup>14</sup> or curcumin-loaded dextran sulphate-chitosan nanoparticles.<sup>15</sup> In recent decades, many novel chemotherapeutic formulations have been developed. These formulations contain chemotherapy inside the vehicle, resulting in less toxicity and better drug penetration into tumor tissue. Biodegradable polymeric nanoparticles are often used to achieve controlled release of drugs in advanced anticancer drug delivery systems.<sup>16-19</sup> Also, some biodegradable polymer-derived drug delivery systems, such as nanoparticles delivering anticancer agents, are commercially available.<sup>20</sup> Poly(caprolactone)-poly(ethylene glycol) (PCL-PEG) copolymers are

\*Corresponding author: Soodabeh Davaran, Email: davaran@tbzmed.ac.ir

©2014 The Authors. This is an Open Access article distributed under the terms of the Creative Commons Attribution (CC BY), which permits unrestricted use, distribution, and reproduction in any medium, as long as the original authors and source are cited. No permission is required from the authors or the publishers.

biodegradable, amphiphilic, easy to produce, and have potential application in drug delivery systems.<sup>21,22</sup> In order to improve therapeutic efficiency of curcumin, various formulations including liposomal curcumin,<sup>23</sup> PEG-curcumin conjugate,<sup>24</sup> and PCL-PEG-PCL nanofibers or micelles encapsulating curcumin have been introduced recently.<sup>25,26</sup> In this contribution, we are aimed to encapsulate curcumin in mPEG-PCL micelles as a promising carrier with sustained release characteristics. In this way, a novel micellar delivery system with mPEG-PCL was synthesized and the release profile of the curcumin from the micelles prepared using the drug-loaded copolymer was evaluated.

## Materials and Methods

### Materials

mPEG (Mn=5000 Da) (Aldrich, St. Louis, USA, CAS.81323),  $\epsilon$ -caprolactone (98% purity) (Acros, New Jersey, USA, CAS.502443), curcumin (Merck, Darmstadt, Germany, Art No. 820354), and stannous 2-ethylhexanoate (Sn(Oct)<sub>2</sub>) (Aldrich, St. Louis, USA, CAS.301100) were all purchased locally. Other chemicals and solvent were from chemical lab purity grades, purchased locally and used as received.

### Synthesis of mPEG-PCL copolymer

The mPEG-PCL copolymer was synthesized by a ring opening polymerization of  $\epsilon$ -caprolactone with mPEG as initial molecule and Sn(Oct)<sub>2</sub> as catalyst. Briefly,  $\epsilon$ -caprolactone (4 g), mPEG (2 g), and Sn(Oct)<sub>2</sub> (0.01 mmol) were heated to 120°C to start polymerization. After 11 h, the resulting polymer was cooled to room temperature, dissolved in chloroform, and precipitated in cold diethyl ether. The copolymer was dried under vacuum at room temperature for 24 h.

### Characterization of mPEG-PCL copolymer

The chemical structure of copolymer was identified by proton nuclear magnetic resonance spectroscopy (<sup>1</sup>H NMR) in CDCl<sub>3</sub> at 400 MHz (Bruker, Avance 400) and Fourier transform infrared spectroscopy (FT-IR) (Bruker, Tensor 27). The average molecular weight and distribution of the mPEG-PCL copolymers were determined by gel permeation chromatography (GPC) (Knaure, Berlin, Germany) equipped with differential refractometric detector and an ultrastyrigel column (4.6×30 mm) (Waters, Milford, USA, model HR 4E). The mobile phase was tetrahydrofuran (THF) with a flow-rate of 1 ml/min and the injection volume was 100  $\mu$ l of stock solutions (0.1-0.5 w/v %). Polymers were characterized by relative elution time to polystyrene monodisperse standards in the range of 4500- 29500 Da (Varian Palo Alto, CA) using the calibration curve obtained before measurements. Differential scanning calorimetry (DSC) (Mettler Toledo, model Star SW 9.30) was used for thermal analysis of the synthesized copolymers. Samples were heated at a rate of 10 °C min<sup>-1</sup> and the data were recorded from 0 to 200 °C.

### Preparation of curcumin-loaded micelles

Curcumin loaded micelles were prepared by nanoprecipitation method using chloroform as the solvent. Briefly, mPEG-PCL copolymer (20 mg), and curcumin (8 mg) were dissolved in 2 ml of chloroform. The solution was, then, injected drop-wise through a syringe (G=22) into 25 ml of distilled water under certain mixing rates and stirred magnetically at room temperature until complete evaporation of the organic solvent which caused the amphiphilic copolymers to self-associate to form the micelles. The resulting micelles were separated by centrifuging at 20000 g for 20min and freeze-dried under a pressure of 14 Pa at -78 °C in order to remove all the residual solvents and to produce the final dried form.

### Characterization of the micelles

#### Particle morphology

The morphology of micelles was determined using atomic force microscopy (AFM) (JPK, Berlin, Germany, model Nano Wizard 2). For AFM sample preparation, micelles were diluted with water and a droplet of 2  $\mu$ L was placed onto a freshly cleaved mica substrate (1 cm<sup>2</sup>) and air-dried. AFM measurements were performed in intermittent contact mode.

#### Determination of particle size

The particle size distribution of the prepared micelles were determined by dynamic light scattering (DLS) using a nano/zetasizer (Malvern Instruments, Worcestershire, UK, model Nano ZS).

#### Stability of micelles

The physical stability of micelles was evaluated by monitoring the particle size distribution of the micelles while suspended in phosphate-buffered solution (PBS, pH=7.4) and kept in ambient temperature at times 0, 15, and 30 days after preparation using the method described in 2.5.2.

#### Determination of loading efficiency

To determine the loading efficiency of the drugs in the micelles, two parameters were determined including the drug loading ratio and efficiency of entrapment. Drug loading ratio was determined as:

$$\%DL = \frac{W_{Drug}}{W_{Micelles}} \times 100 \quad (1)$$

Where DL% is the drug loading ratio (percent), and W<sub>drug</sub> and W<sub>micelles</sub> represent the weight of the entrapped drug, and the total weight of the corresponding drug-entrapped micelles, respectively.

For determination of the drug loading ratio, 1 mg of the final freeze-dried nanodispersion was dissolved in 1 mL of chloroform, and the drug content was measured spectrophotometrically (Thermo Fisher Scientific, USA, Madison, model GENESYS™ 10S) at wavelengths of 425nm.

Efficiency of entrapment was determined in reference to loading ratio and total dried nanodispersion weight obtained using the following equation:

$$EE\% = \frac{(W_{t\text{ micelles}} \times DL)}{W_{\text{feed drug}}} \times 100 \quad (2)$$

Where EE% is the efficiency of entrapment (percent), and  $W_{t\text{ micelles}}$  and  $W_{\text{feed drug}}$  stand for the total mass of powders obtained after freeze-drying and the drug fed initially in the micelles preparation step, respectively.

#### FTIR analysis

Using FTIR analysis, it is possible to obtain some information about the occurrence of possible interaction(s) between substances involved in a nanocarrier system. Generally, the interaction between drug and polymer is investigated through the band shifts exerted by the functional groups as well as through broadening in IR spectra compared to their individual spectra. To confirm the presence of any interactions between drug and polymer, the FTIR spectra of solid micelles were compared with pure drug and individual polymers. Freeze-dried samples were pressed to form the standard disks and the FTIR spectra of the KBr disks were recorded using the aforementioned instrument from 600 to 4000  $\text{cm}^{-1}$ .

#### DSC analysis

Any possible drug-polymer interaction(s) as well as the physical changes occurred on the drug or polymer can be studied using the thermal analysis. DSC analysis was carried out on pure drug and drug-loaded micelles. Samples were heated at a rate of 10  $^{\circ}\text{C min}^{-1}$  and the data were recorded from 0 to 200  $^{\circ}\text{C}$ .

#### Drug release study

This test was carried out to evaluate the release behavior of curcumin from micellized copolymer. Briefly, 5 mg of freeze-dried drug-loaded carriers were dispersed in 2 ml phosphate-buffered saline (PBS) containing 5% (v/v) Tween 80 and the resulting suspension was placed within a dialysis sac (Mw 12 kDa) and incubated at 37  $^{\circ}\text{C}$  while immersed in 15 ml of PBS. Then, at predetermined time intervals, 2 ml of the dialysate was taken out and replaced by 2 ml fresh PBS. The concentration of curcumin in the dialysate was determined by high performance liquid

chromatography (HPLC). The mobile phase consisted of methanol and 5% (w/v) acetic acid at the volume ratio of 70:30, and was delivered at a flow rate of 1.0 ml/min using a double-reciprocating pump and the analysis wavelength was at 420 nm (Waters, MA, USA, model Breeze). The sample was injected through a 50  $\mu\text{L}$  sample loop. A  $\text{C}_{18}$  analytical column (250mm $\times$ 4.6mm, particle size 5 $\mu\text{m}$ ; Perfectsill, MZ-Analysentechnik, Germany) equipped by a guard column of the same packing was used. The calibration curve for curcumin was linear over the concentration range of 0.0016-0.125 mg/ml. All the release studies were carried out in triplicate. In order to study the pH-dependency of the drug release, the experiments were also carried out, as specified earlier, using PBS at a pH of 5.5. To investigate the drug release behavior of carriers while incubated in real human plasma, the release experiments were repeated in plasma of a healthy male volunteer in the same condition except that the samples were incubated in plasma instead of PBS.

## Results

### Synthesis and characterization of mPEG-PCL copolymer

mPEG-PCL di-block copolymer was synthesized using the ring-opening polymerization of caprolactone in presence of mPEG, whose hydroxyl end group initiated the ring opening (Figure 1). The structure and composition of the synthesized mPEG-PCL di-block copolymer was determined by HNMR spectroscopy in  $\text{CDCl}_3$ , as shown in Figure 2. The presence of methylenes ( $\text{CH}_2$ ) in PCL was observed around 1.3 ppm, 1.6 ppm, 2.2 ppm and 4.06 ppm, the methoxy and methylene protons in methoxy ( $\text{OCH}_3$ ) and methylene ( $\text{CH}_2$ ) groups of PEG were around 3.38 and 3.64 ppm, respectively. Table 1 shows the characteristics of synthesized copolymer. FT-IR spectrum of mPEG-PCL copolymer is shown in Figure 3. In the spectrum shown, the sharp and intense bands at 1722  $\text{cm}^{-1}$  and 1106  $\text{cm}^{-1}$  were awardable to the presence of carboxylic ester ( $\text{C}=\text{O}$ ) and ether ( $\text{C}-\text{O}$ ) groups, thereby indicating that the formation of mPEG-PCL copolymer has occurred successfully. GPC results showed that the weight- and number-based average molecular weights of copolymer were 22.7 and 25.6 KDa, respectively (Figure 4).<sup>27,28</sup>

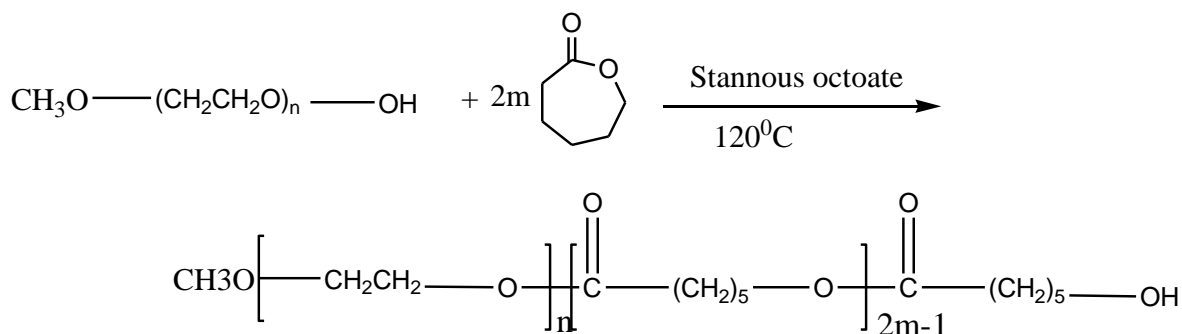


Figure 1. Schematic synthesis route of mPEG-PCL copolymer.

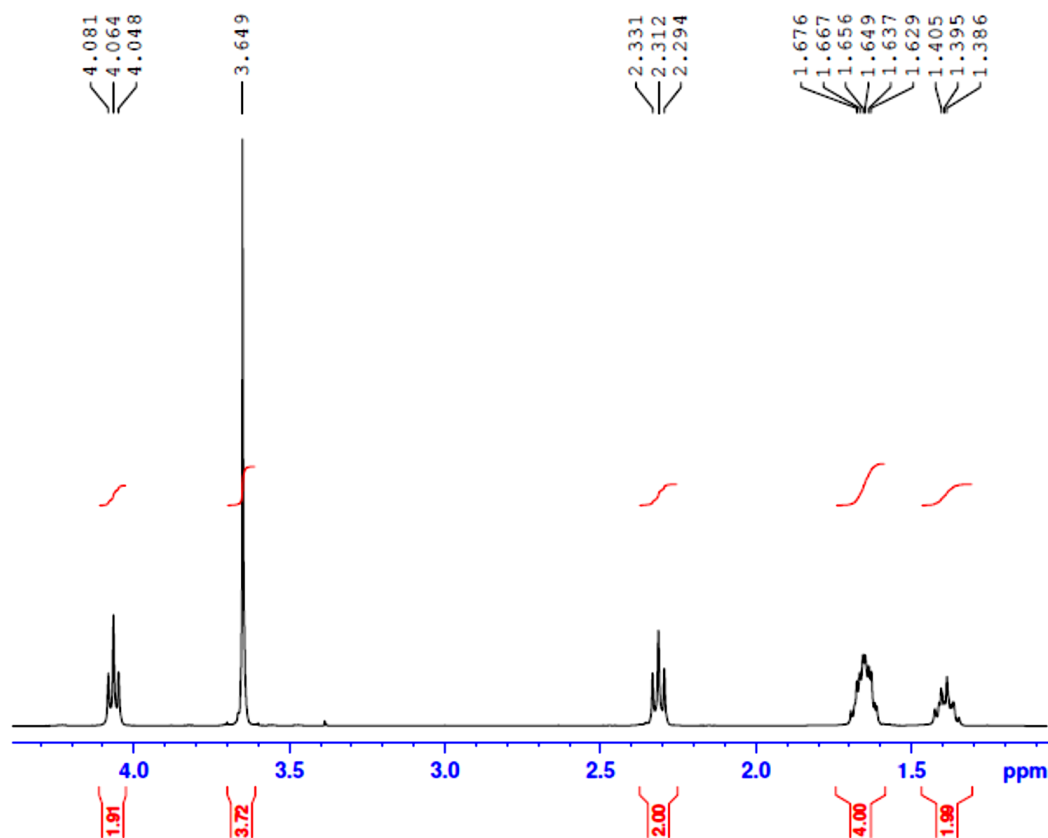


Figure 2.  $^1\text{H}$  NMR spectrum of mPEG–PCL di-block copolymer in  $\text{CDCl}_3$ .

Table 1. Molecular characteristics of the synthesized copolymer

Copolymer	CL/EG feed	$M_n$ (KDa) <sup>a</sup>	$M_w$ (KDa) <sup>a</sup>	PdI <sup>b</sup>	$T_m$ (°C) <sup>c</sup>	DP <sub>PEG</sub>	DP <sub>PCL</sub> <sup>d</sup>
mPEG–PCL	0.5	22.7	25.6	1.13	58.68	136.36	157

a: Determined by GPC analysis using narrow molecular weight polystyrene standards

b:  $M_w/M_n$  = Polydispersity index of the polymers (PdI) determined by GPC analysis

c: Calculated from the first run of DSC as half of the extrapolated tangents

d: DP: degree of polymerization

### Preparation and characterization of copolymeric micelles

The formation of micellar nanostructures was confirmed by AFM. Apparently, mPEG–PCL micelles showed a homogeneous spherical morphology, as expected (Figure 5). The size of nanoparticles was measured by dynamic light scattering technique. As shown in Figure 6, the z-average and zeta potential of curcumin loaded mPEG–PCL micelles were found to be about 128 nm and -12 mv, with their corresponding PDI being 0.166. The micelle size observed by AFM was about 73.8 nm, a little smaller than that determined by DLS. It can be explained by the fact that the micelle diameter determined by DLS represents the hydrodynamics diameter while that obtained by AFM is related to the collapsed micelles after water evaporation. The loading ratio and encapsulation efficiencies of curcumin loaded to mPEG–PCL micelles were determined to be  $23\% \pm 1.25\%$  and  $88\% \pm 3.32\%$ , respectively.

### FTIR analysis

Figure 7 illustrates the FTIR spectra of mPEG–PCL copolymer, curcumin, and curcumin-loaded mPEG–PCL micelles. The FTIR spectrum of curcumin shows characteristic bands appeared at  $3515.77\text{ cm}^{-1}$  (O–H, stretching) for phenolic hydroxyl group,  $1630.97\text{ cm}^{-1}$  (C=C, stretching),  $1512.94\text{ cm}^{-1}$  (C=C band of benzene), and  $856.38\text{ cm}^{-1}$  (C–H, stretching of aromatic ring) (Figure 7). Comparing these data with the drug-loaded micelles spectrum exhibits the presence of curcumin characteristic peaks in the spectrum of micelles which could demonstrate the successful loading of curcumin in the nanoparticles. The most striking feature of the FTIR spectra of micelles was the blue shift of the C=O vibration, from  $1728.68$  to  $1730.56\text{ cm}^{-1}$  for drug-loaded mPEG–PCL micelles compared to the copolymer spectrum. The shift in the micelles spectrum indicates that there exist some form(s) of association between curcumin and C=O functional group of copolymer.<sup>29</sup>

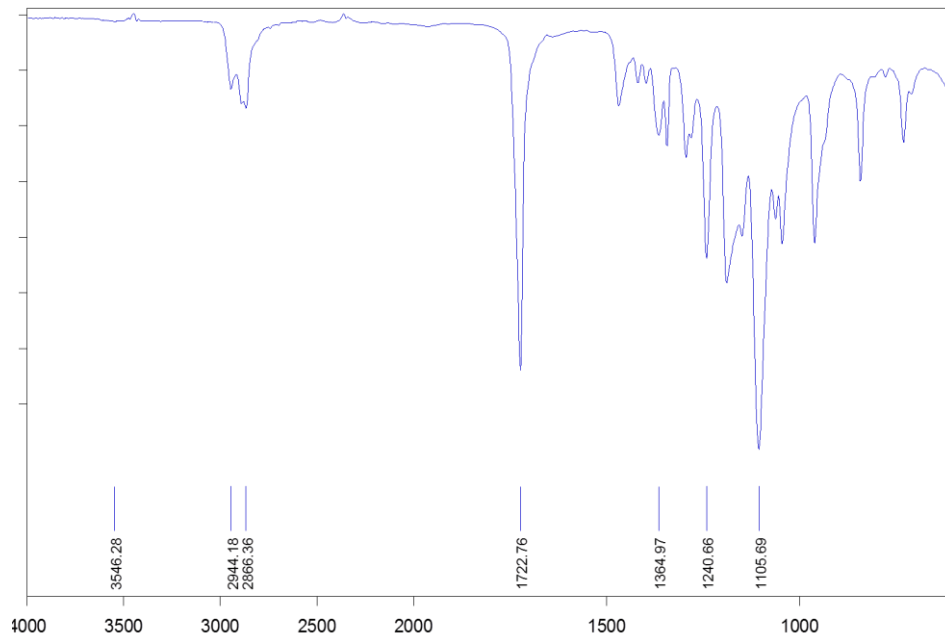


Figure 3. FT-IR spectrum of mPEG-PCL di-block copolymer in

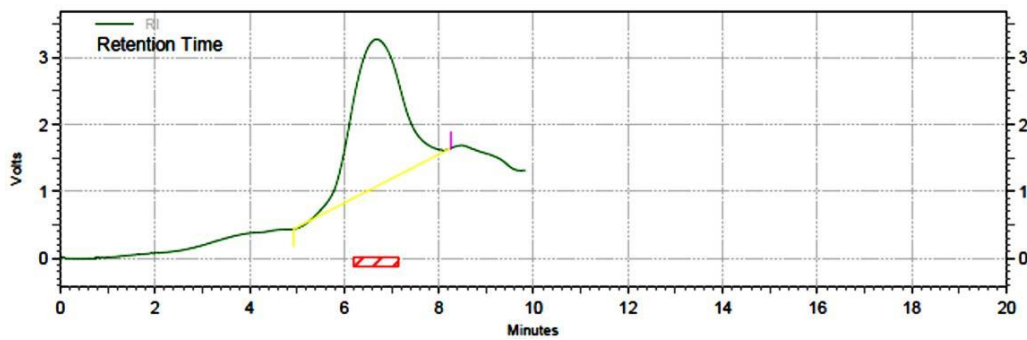


Figure 4. GPC spectrum of mPEG-PCL copolymer.

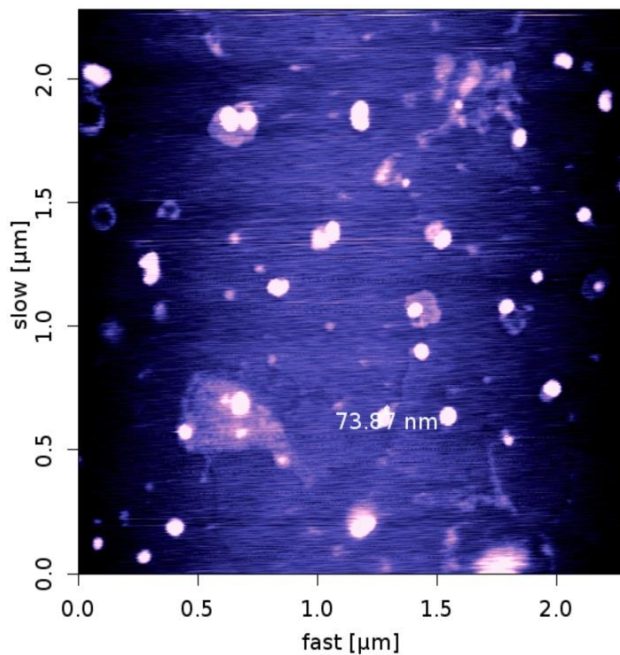


Figure 5. AFM image of micelles

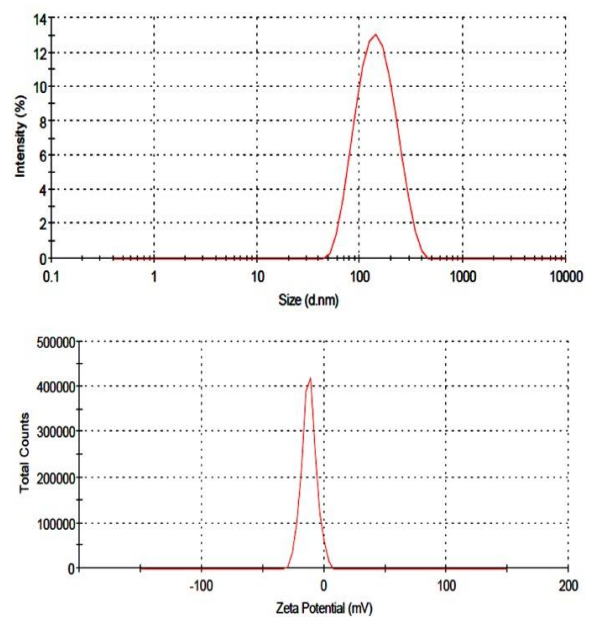
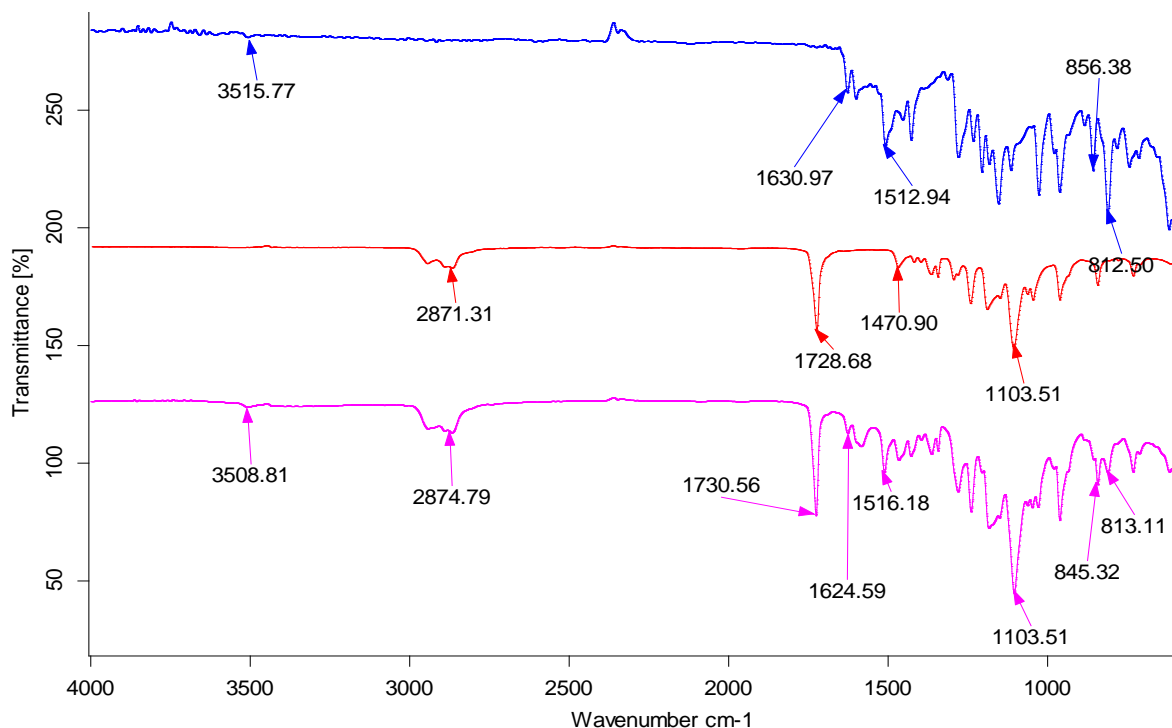


Figure 6. Particle size distribution and zeta potential of mPEG-PCL-DOX micelles (a) particle size distribution (b) zeta potential



**Figure 7.** FT-IR spectra of (a) curcumin, (b) mPEG-PCL and, (c) CUR-mPEG-PCL micelles.

### DSC analysis

Figure 8 shows the DSC thermograms corresponding to mPEG-PCL copolymer, curcumin and micelles loaded by curcumin. The thermogram of mPEG-PCL copolymer displayed an endothermic peak at 58.68 °C which is indicative for the melting of the crystalline PCL segment of copolymer, the thermogram of curcumin displayed an endothermic peak at 176.71 °C and micelles displayed two endothermic peaks at 49.09 °C and 175.55 °C which stand for the melting of copolymer and curcumin association in the form of micelles. This endothermic peak of micelles presumably confirms a physical interaction between copolymer and curcumin upon loading of the drug in micelles, since the melting point of PCL micelles was lower than melting point of both copolymer (58.68 °C) and pure curcumin (176.71 °C).

### In vitro release of curcumin

#### The impact of different release media on drug release from micelles

In order to examine the influence of the chemical and biochemical factors on the release of curcumin from micelles, the release study was carried out on drug-loaded micelles in neutral and acidified PBS solution (pH=5.5) as well as the freshly prepared human plasma withdrawn from a volunteer. Figure 9 shows the release profiles of curcumin from the drug-loaded micelles, at pH 7.4, 5.5, and plasma. As expected, no considerable initial burst curcumin release was observed from the micelles. As shown in Figure 9, the percentage of curcumin released from the micelles slightly increased as the pH value decreased from 7.4 to 5.5. For example,

after 96 h incubation, the amounts of curcumin released in the media with pH values of 7.4, 5.5 and human plasma were about 66, 78, and 67 %, respectively. This fact may be due to the physical loading of curcumin to the micelles. The results revealed the maximum drug release percent attainable after a period of 120 h in PBS pH=7.4, 5.5 and plasma were 73.13%, 84.68%, and 79.78%, respectively. The sustained release of curcumin can be attributed to the entrapment of curcumin in core of micelles. Therefore, our copolymeric micelles can be regarded as highly attractive nanocarriers for both time-controlled drug delivery for hydrophobic drugs for the achievement of different therapeutic objectives.

### Physical stability of micelles

In the clinical administration of nanoparticle dispersions, the stability of the sizes of the nanocarriers is of great importance both as a measure of the particle structure integrity and as an indicator of the possible inter-particular associations (aggregation). For this purpose, the particle size stability was monitored in this study over a 30-days course. The variation of the sizes of micelles as a function of incubation time is shown in Table 2. As it can be seen, the size of all micelles was increased slightly throughout the measurement period. This observation cannot be a sign of aggregation, which usually leads to several fold increases. Probably some kind of copolymer swelling and/or hydration as a result of presence of the hydrophilic PEG portions in micelles surfaces can be responsible for this event.

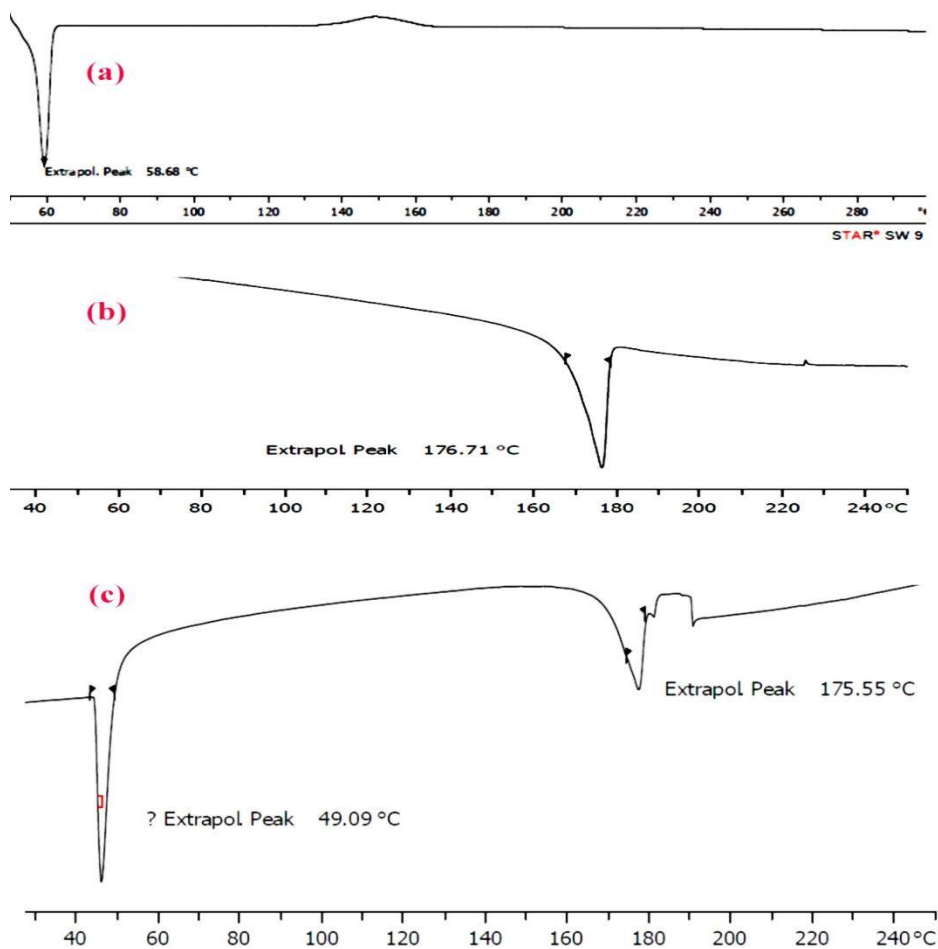


Figure 8. DSC spectra of (a) mPEG-PCL,(b) Curcumin and (c)CUR-mPEG-PCL micelles.

Table 2. Stability of nanoparticles suspension

micelles	Mean size of micelles immediately after preparation (nm)	Mean size of micelles after 15 day (nm)	Mean size of micelles after 30 days (nm)
CUR-mPEG-PCL-DOX micelles	128	145	180

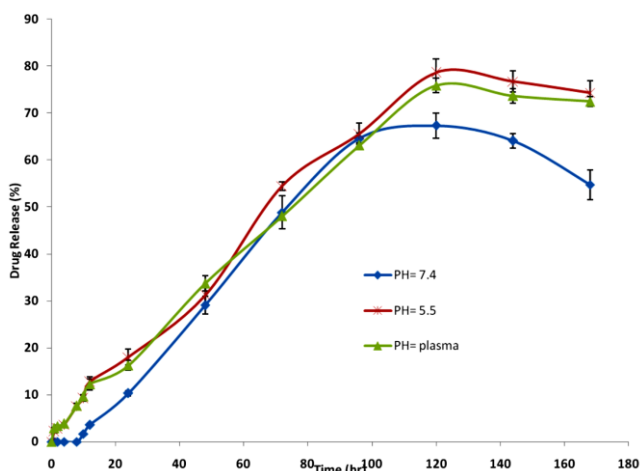


Figure 9. The release profiles of curcumin from CUR-mPEG-PCL micelles in different release media (a) PH= 7.4, (b) plasma, (c) pH=5.5.

### Discussion

Curcumin, a biologically active component of turmeric, has been used as an herbal medicine for the treatment of inflammatory disorders, cancer, acquired immune deficiency syndrome, and other diseases for a long time.<sup>30-33</sup> It has been found to have preventive and therapeutic effects in various cancers, and has been confirmed to be a potent chemosensitizer.<sup>34</sup> The problem with using curcumin is that it is poorly soluble in water and is easily degraded by the body. Thus, curcumin cannot be used via the intravenous route, where it could possibly exert a maximal pharmacological effect. mPEG-PCL was employed in this study to prepare micelles, as described. To overcome the poor water-solubility of curcumin, curcumin was encapsulated into MPEG-PCL micelles by a self-assembly method, producing curcumin /MPEG-PCL micelles. Amphiphilic nature of mPEG-

PCL with hydrophilic PEG and hydrophobic PCL blocks provides an opportunity to form micelles in water. This behavior can be explained as a consequence of copolymer self-assembly into micellar structure because of its amphiphilic nature which, subsequently forces the hydrophilic PEG segments to serve as hydrophilic shell and the hydrophobic PCL segments to become the micellar core.

The size of curcumin /mPEG-PCL micelles were about 74 nm in diameter. Also, curcumin /mPEG-PCL micelles showed drug loading of  $23\% \pm 1.25\%$  and a high encapsulation efficiency of  $88 \pm 3.32\%$ , making this an aqueous formulation of curcumin. In addition, the curcumin /mPEG-PCL micelles had a negative surface charge of -12 mV, which increased the circulation time of the drug. Surface charge is important in determining whether the nanoparticles will cluster in blood flow or will adhere to or interact with oppositely charged cell membrane.<sup>35</sup> The plasma and blood cells always had a negative charge; nanoparticles with slight negative surface charge may minimize nonspecific interaction with these components through electrostatic interactions.<sup>36-38</sup> The curcumin /MPEG-PCL micelles were able to slowly release curcumin (Figure 9). The sustained release of curcumin from MPEG-PCL micelles might be due to the diffusion of curcumin from micelles and the degradation or hydrolysis of micelles. In this work, we used mPEG-PCL micelles to encapsulate curcumin. In the preparation process, curcumin and mPEG-PCL diblock copolymer mixture was first dissolved in chloroform solution, followed by evaporating the organic solvent. Then, the amphiphilic MPEG-PCL copolymers self-assembled into supramolecular arrangements possessing a hydrophobic inner core and a hydrophilic shell in water, and curcumin self-assembled into the hydrophobic core of the micelles because of its hydrophobicity. The preparation procedure was simple and easy to scale up. These mPEG-PCL micelles are biodegradable, biocompatible, amphiphilic, stable in blood, nontoxic, nonimmunogenic, non-inflammatory, and small in size; these make mPEG-PCL micelles an excellent candidate for drug-delivery systems.<sup>35</sup> Thus, mPEG-PCL micelle-encapsulated curcumin might be an interesting formulation to improve drug efficacy. In summary, mPEG-PCL micelles were used to encapsulate curcumin, creating curcumin /mPEG-PCL micelles. The curcumin /mPEG-PCL micelles improved the water solubility of curcumin. and may have potential application in cancer treatment.

### Conclusion

Methoxypoly(ethylene glycol)-poly caprolactone-(mPEG-PCL) copolymer was synthesized and characterized by HNMR, FTIR, DSC and GPC techniques. Then, the mPEG-PCL copolymer were self-assembled into micelles in aqueous solution in presence of curcumin. The resulting micelles were characterized by various techniques such as DLS and AFM. The

encapsulation efficiency of curcumin was  $88 \pm 3.32\%$ . The results revealed that the micelles formed had spherical structure with size of 73.8 nm. *In vitro* release of curcumin from curcumin-entrapped micelles was clearly sustained in all the media tested for this purpose, with the apparent release plateau reached late at about 130 h.

### Acknowledgments

This work has been supported financially by Faculty of Pharmacy, Tabriz University of Medical Sciences under a Ph.D. thesis proposal (No. 81). The authors are also most grateful for the continuing financial support of this research project by Zanjan University of Medical Sciences, Zanjan, Iran.

### Conflict of Interest

The authors declare that they have no conflict of interest.

### References

1. Sun YM, Zhang HY, Chen DZ, Liu CB. Theoretical elucidation on the antioxidant mechanism of curcumin: a DFT study. *Org Lett* 2002;4(17):2909-11.
2. Han S, Yang Y. Antimicrobial activity of wool fabric treated with curcumin. *Dyes Pigments* 2005;64(2):157-61.
3. Kohli K, Ali J, Ansari MJ, Raheman Z. Curcumin: a natural antiinflammatory agent. *Ind J Pharmacol* 2005;37(3):141-7.
4. Panchatcharam M, Miriyala S, Gayathri VS, Suguna L. Curcumin improves wound healing by modulating collagen and decreasing reactive oxygen species. *Mol Cell Biochem* 2006;290(1-2):87-96.
5. Sun A, Shoji M, Lu YJ, Liotta DC, Snyder JP. Synthesis of EF24-tripeptide chloromethyl ketone: a novel curcumin-related anticancer drug delivery system. *J Med Chem* 2006;49(11):3153-8.
6. Somasundaram S, Edmund NA, Moore DT, Small GW, Shi YY, Orłowski RZ. Dietary curcumin inhibits chemotherapy-induced apoptosis in models of human breast cancer. *Cancer Res* 2002;62(13):3868-75.
7. Aggarwal BB, Shishodia S, Takada Y, Banerjee S, Newman RA, Bueso-Ramos CE, et al. Curcumin suppresses the paclitaxel-induced nuclear factor-kappaB pathway in breast cancer cells and inhibits lung metastasis of human breast cancer in nude mice. *Clin Cancer Res* 2005;11(20):7490-8.
8. Tonnesen HH, Karlsen J. Studies on curcumin and curcuminoids. VI. Kinetics of curcumin degradation in aqueous solution. *Z Lebensm Unters Forsch* 1985;180(5):402-4.
9. Tonnesen HH, Karlsen J, Van Henegouwen GB. Studies on curcumin and curcuminoids. VIII. Photochemical stability of curcumin. *Z Lebensm Unters Forsch* 1986;183(2):116-22.
10. Yen FL, Wu TH, Tzeng CW, Lin LT, Lin CC. Curcumin nanoparticles improve the physicochemical



- properties of curcumin and effectively enhance its antioxidant and antihepatoma activities. *J Agric Food Chem* 2010;58(12):7376-82.
11. Tonnesen HH. Solubility, chemical and photochemical stability of curcumin in surfactant solutions. Studies of curcumin and curcuminoids, XXVIII. *Die Pharmazie* 2002;57(12):820-4.
  12. Tonnesen HH, Masson M, Loftsson T. Studies of curcumin and curcuminoids. XXVII. Cyclodextrin complexation: solubility, chemical and photochemical stability. *Int J Pharm* 2002;244(1-2):127-35.
  13. Lin CC, Lin HY, Chen HC, Yu MW, Lee MH. Stability and characterisation of phospholipid-based curcumin-encapsulated microemulsions. *Food Chem* 2009;116(4):923-8.
  14. Anitha A, Maya S, Deepaa N, Chennazhi KP, Nair SV, Tamura H, et al. Efficient water soluble O-carboxymethyl chitosan nanocarrier for the delivery of curcumin to cancer cells. *Carbohydr Polym* 2011;83(2):452-61.
  15. Anitha A, Deepagan VG, Divya Rani VV, Menon D, Nair SV, Jayakumar R. Preparation, characterization, in vitro drug release and biological studies of curcumin loaded dextran sulphate-chitosan nanoparticles. *Carbohydr Polym* 2011;84(3):1158-64.
  16. Shutava TG, Balkundi SS, Vangala P, Steffan JJ, Bigelow RL, Cardelli JA, et al. Layer-by-Layer-Coated Gelatin Nanoparticles as a Vehicle for Delivery of Natural Polyphenols. *ACS Nano* 2009;3(7):1877-85.
  17. Shieh YA, Yang SJ, Wei MF, Shieh MJ. Aptamer-based tumor-targeted drug delivery for photodynamic therapy. *ACS Nano* 2010;4(3):1433-42.
  18. Wang T, He N. Preparation, characterization and applications of low-molecular-weight alginate-oligochitosan nanocapsules. *Nanoscale* 2010;2(2):230-9.
  19. He N, Wang T, Jiang L, Wang D, Hu Y, Zhang L. Therapy for cerebral ischemic injury with erythropoietin-containing nanoparticles. *J Nanosci Nanotechnol* 2010;10(8):5320-3.
  20. Wang X, Yang L, Chen ZG, Shin DM. Application of nanotechnology in cancer therapy and imaging. *CA Cancer J Clin* 2008;58(2):97-110.
  21. Wei X, Gong C, Gou M, Fu S, Guo Q, Shi S, et al. Biodegradable poly(epsilon-caprolactone)-poly(ethylene glycol) copolymers as drug delivery system. *Int J Pharm* 2009;381(1):1-18.
  22. Gou M, Wei X, Men K, Wang B, Luo F, Zhao X, et al. PCL/PEG copolymeric nanoparticles: potential nanoplatforams for anticancer agent delivery. *Curr Drug Targets* 2011;12(8):1131-50.
  23. Shi HS, Gao X, Li D, Zhang QW, Wang YS, Zheng Y, et al. A systemic administration of liposomal curcumin inhibits radiation pneumonitis and sensitizes lung carcinoma to radiation. *Int J Nanomedicine* 2012;7:2601-11.
  24. Safavy A, Raisch KP, Mantena S, Sanford LL, Sham SW, Krishna NR, et al. Design and development of water-soluble curcumin conjugates as potential anticancer agents. *J Med Chem* 2007;50(24):6284-8.
  25. Guo G, Fu S, Zhou L, Liang H, Fan M, Luo F, et al. Preparation of curcumin loaded poly(epsilon-caprolactone)-poly(ethylene glycol)-poly(epsilon-caprolactone) nanofibers and their in vitro antitumor activity against Glioma 9L cells. *Nanoscale* 2011;3(9):3825-32.
  26. Men K, Gou ML, Guo QF, Wang XH, Shi S, Kan B, et al. A novel drug and gene co-delivery system based on Poly(epsilon-caprolactone)-Poly(ethylene glycol)-Poly(epsilon-caprolactone) grafted polyethyleneimine micelle. *J Nanosci Nanotechnol* 2010;10(12):7958-64.
  27. Yodthong B. Surfactant-Free Nanospheres of m/PEG-PCL for controlled release of ibuprofen. *J Appl Sci* 2009;9(12):2278-9.
  28. Weihui X, Weipu Z, Zhiquan S. Synthesis, isothermal crystallization and micellization of mPEG-PCL diblock copolymers catalyzed by yttrium complex. *Polymer* 2007;48(23):6791-8.
  29. Duan J, Mansour HM, Zhang Y, Deng X, Chen Y, Wang J, et al. Reversion of multidrug resistance by co-encapsulation of doxorubicin and curcumin in chitosan/poly(butyl cyanoacrylate) nanoparticles. *Int J Pharm* 2012;426(1-2):193-201.
  30. Di Santo R, Costi R, Artico M, Ragno R, Greco G, Novellino E, et al. Design, synthesis and biological evaluation of heteroaryl diketohexenoic and diketobutanoic acids as HIV-1 integrase inhibitors endowed with antiretroviral activity. *Farmaco* 2005;60(5):409-17.
  31. Abouzid KA, Khalil NA, Ahmed EM, Zaitone SA. Synthesis and biological evaluation of new heteroaryl carboxylic acid derivatives as anti-inflammatory-analgesic agents. *Chem Pharm Bull (Tokyo)* 2013;61(2):222-8.
  32. Xu Y, Ku B, Tie L, Yao H, Jiang W, Ma X, et al. Curcumin reverses the effects of chronic stress on behavior, the HPA axis, BDNF expression and phosphorylation of CREB. *Brain Res* 2006;1122(1):56-64.
  33. Shi M, Cai Q, Yao L, Mao Y, Ming Y, Ouyang G. Antiproliferation and apoptosis induced by curcumin in human ovarian cancer cells. *Cell Biol Int* 2006;30(3):221-6.
  34. Sen GS, Mohanty S, Hossain DM, Bhattacharyya S, Banerjee S, Chakraborty J, et al. Curcumin enhances the efficacy of chemotherapy by tailoring p65NFkappaB-p300 cross-talk in favor of p53-p300 in breast cancer. *J Biol Chem* 2011;286(49):42232-47.
  35. Kumari A, Yadav SK, Yadav SC. Biodegradable polymeric nanoparticles based drug delivery systems. *Colloids Surf B Biointerfaces* 2010;75(1):1-18.
  36. Turner MR, Clough G, Michel CC. The effects of cationised ferritin and native ferritin upon the

- filtration coefficient of single frog capillaries. Evidence that proteins in the endothelial cell coat influence permeability. *Microvasc Res* 1983;25(2):205-22.
37. Vink H, Duling BR. Identification of distinct luminal domains for macromolecules, erythrocytes, and leukocytes within mammalian capillaries. *Circ Res* 1996;79(3):581-9.
38. Dellian M, Yuan F, Trubetskoy VS, Torchilin VP, Jain RK. Vascular permeability in a human tumour xenograft: molecular charge dependence. *Br J Cancer* 2000;82(9):1513-8.